Nuclear Physics **A509** (1990) 800–822
North-Holland

COHERENT ELECTROMAGNETIC EXCITATION AND DISINTEGRATION OF RELATIVISTIC NUCLEI PASSING THROUGH CRYSTALS

Yu.L. PIVOVAROV[1]

The Niels Bohr Institute, University of Copenhagen Ø, Blegdamsvej 17, DK-2100, Denmark

A.A. SHIROKOV and S.A. VOROBIEV

Nuclear Physics Institute, 634050 Tomsk, P.O. Box 25, USSR

Received 17 June 1988
(Revised 21 July 1989)

Abstract: The energy dependence of electromagnetic excitation and electromagnetic disintegration cross sections for relativistic nuclei passing through crystals is investigated both theoretically and by means of computer simulation. For electromagnetic excitation, resonant peaks are found at definite energy values. An increase of electromagnetic excitation and disintegration cross sections in crystals at very high energies is found to be due to coherent addition of amplitudes. Numerical results are presented for the electric dipole excitation of fluorine nuclei and electromagnetic deuteron disintegration.

1. Introduction

Besides nuclear reactions, heavy-ion collisions lead to electromagnetic excitation (EE) or electromagnetic disintegration (ED) of nuclei. These phenomena have been studied in detail both experimentally and theoretically at non-relativistic energies [1]) and now are under study at high energies [2-4]) on the new heavy-ion accelerators, with ion energies up to 200 GeV/nucleon. Both the developed theory and experiments usually deal with the interaction of relativistic nuclei with amorphous targets. Recent experiments at GANIL [5]) have shown the possibility of relativistic nuclei channeling in crystals. Relativistic channeling has been previously studied for π and K mesons, electrons and positrons and leads to various new effects, e.g. channeling radiation [6]) and pair production [7]) in the electric fields of the crystal planes or axes. Channeling of the positively charged particles is, as is known (see e.g. ref. [8])), motion along specific trajectories between the crystal planes or axes. Nuclear collisions with small impact parameters are suppressed at channeling, therefore a relative increase of the electromagnetic channel of the nucleus–nucleus interactions at high energies should be expected. Since the electric field of the crystal is periodic, it has to affect the EE and ED processes in a specific way, as compared to an amorphous target.

[1] On leave from Nuclear Physics Institute, 634050 Tomsk, P.O. Box 25, USSR.

Let us consider qualitatively the possible effects in the electromagnetic excitation of relativistic nuclei passing through a crystal. The periodic potential of the crystal can be represented in the form:

$$\varphi(\boldsymbol{r}) = \sum_a \varphi(\boldsymbol{r} - \boldsymbol{r}_a) = \sum_k e^{-i\boldsymbol{k}\cdot\boldsymbol{r}} \varphi_k , \tag{1}$$

where $\boldsymbol{k} = (2\pi l/a_x, 2\pi m/a_y, 2\pi n/a_z)$ is a reciprocal lattice vector and a_x, a_y, a_z are the lattice periods. Let us consider the case when the relativistic nucleus penetrates through the crystal along the straight-line trajectory $\boldsymbol{r}(t) = \boldsymbol{v} \cdot t$, where $\boldsymbol{v}$ is the mean velocity of the nucleus. The electromagnetic scalar and vector potentials appearing in the rest frame of the nucleus depend on the time t' through $\exp[i\gamma(\boldsymbol{v}\cdot\boldsymbol{k})t']$, where $\gamma = (1-\beta^2)^{-1/2}$ and $\beta = v/c$. It follows immediately, under the condition

$$\gamma(\boldsymbol{v}\cdot\boldsymbol{k}) = \omega_0 , \tag{2}$$

where ω_0 is the transition frequency between the nuclear levels, that resonant excitation may occur. In this case the amplitude of the process becomes proportional to the number N of atoms along the trajectory of the nucleus in the crystal and the excitation probability becomes proportional to the square of the number of atoms N^2. Below we denote this process as the coherent resonant excitation (coherent but non-resonant excitation is considered in sect. 3). In addition to the condition (2) one should require $|\varphi_k|^2 \neq 0$ and we obtain, for example, for a monoatomic crystal a system of equations, which determines the conditions of the resonant coherent EE of relativistic nuclei:

$$\gamma(\boldsymbol{v}\cdot\boldsymbol{k}) = \omega_0 , \qquad |S(\boldsymbol{k})|^2 \neq 0 , \tag{3}$$

where $S(\boldsymbol{k})$ is the structure factor [10]) of the crystal. The general conditions (3) are more simple in the two following cases:

(i) $\boldsymbol{v}\cdot\boldsymbol{k}_x = \boldsymbol{v}\cdot\boldsymbol{k}_y = 0$ - the mean velocity of the nucleus is perpendicular to the plane of the reciprocal vectors $(\boldsymbol{k}_x, \boldsymbol{k}_y)$ and is parallel to the crystallographic axis. The corresponding perturbation frequency $\omega_n = (2\pi\gamma v/a_z)n$, $n = \pm 1, \pm 2, \ldots$ is proportional to the transit frequency of the nucleus between two atoms in the crystal string calculated in the rest frame (see fig. 1a). This case is usually called axial channeling.

(ii) $\boldsymbol{v}\cdot\boldsymbol{k}_y = 0$ - the mean velocity of the nucleus is perpendicular to the chain of reciprocal lattice vectors $\boldsymbol{k}_y$ and is parallel to the system of the crystallographic planes (fig. 1b). In this case the perturbation frequency $\omega_{nl} = \omega_n + \omega_l$, where $\omega_n = (2\pi\gamma v_z/a_z)n$, $n = \pm 1, \pm 2, \ldots$ is proportional to the transit frequency between two atoms in the atomic strings along OZ axis and $\omega_l = (2\pi\gamma v_x/a_x)l$, $l = \pm 1, \pm 2, \ldots$ is proportional to the transit frequency between the neighbouring strings. This case is usually called planar channeling.

Thus, the periodic electric field of the crystal can lead to the resonant EE of the compound particle passing through the crystal.

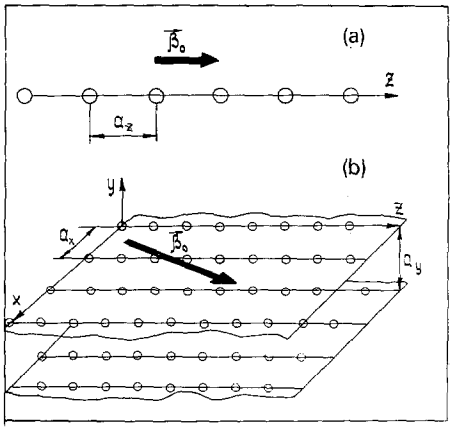

Fig. 1. The schematic drawing of the nucleus motion in the crystal under axial (a) and planar (b) channeling. In the case (a) the incident nucleus velocity $v(0) = c\beta_0$ is parallel to the crystallographic axis and in the case (b), $v(0)$ is parallel to the crystallographic planes.

Okorokov was the first [11,12]) who payed attention to the possibility of a resonant excitation of ions and nuclei under axial channeling. The theory of resonant coherent excitation of electronic levels of channeled ions was developed in the refs. [13-15]). The experimental investigations led to reliable observation of this effect (see e.g. ref. [20]) and references therein). In our papers [9,16-19]) the relativistic nucleus - crystal interaction was considered at first theoretically, and the cross sections of the coherent EE and coherent ED were estimated using the method of virtual photons. The resonant coherent EE cross section in crystals was estimated for $\gamma < 20$ in refs. [17,18]) and for $\gamma \gg 10^2$ in ref. [19]). The coherent ED cross section was estimated for $\gamma < 10^2$ in refs. [9,16]).

The purpose of this paper is to study the energy dependence of the coherent EE and coherent ED cross section over a wide range of nuclear energies. The space-time approach to the interpretation of the process of the coherent EE and ED in the crystal is reported, too. A new method of calculation of nuclear EE cross section in a crystal is developed. It is based on computer simulation of nuclear trajectories in crystals. The simulation results confirm suggestion about the possibility of resonant excitation.

2. Virtual photons under axial channeling

Let us consider a relativistic nucleus passing along a straight-line trajectory parallel to a crystal axis, fig. 1a. The range of validity of the straight-line trajectory approach is discussed below. Hoffmann and Baur showed [21]), that for the Coulomb potential both the perturbation theory (Winther-Alder method [2])) and the virtual photon method (Weizsacker-Williams method [22])) lead exactly to the same results in the calculation of the dipole EE and ED of relativistic nuclei. As one can show, the

same is true for the collisions of relativistic nuclei with an arbitrary electromagnetic scalar potential. Although both approaches are equivalent, the WW method is more convenient for the study of the energy dependence of coherent EE and ED cross sections.

Let $\boldsymbol{b}$ be the impact parameter of the collision of the nucleus with the atom during the straight-line motion with $\gamma \gg 1$. According to the WW method, we can replace the electromagnetic nucleus-atom interaction by the interaction of the nucleus with the flux of virtual photons (VP) belonging to the target atom in the rest frame of the nucleus. The spectral density of the electric dipole VP flux depends on the impact parameter $b = |\boldsymbol{b}|$ and for arbitrary atomic potential it has the form:

$$\frac{\mathrm{d}n}{\mathrm{d}\omega}(\omega, \boldsymbol{b}) = \frac{c}{\hbar\omega v^2}\left\{\left|\frac{\partial \mathcal{J}(\omega, \boldsymbol{b})}{\partial \boldsymbol{b}}\right|^2 + \left(\frac{\omega}{\gamma^2 v}\right)^2 \left|\mathcal{J}(\omega, \boldsymbol{b})\right|^2\right\},$$

$$\mathcal{J}(\omega, \boldsymbol{b}) = \int \frac{\mathrm{d}^2 \boldsymbol{k}_\perp}{(2\pi)^3} \mathrm{e}^{i\boldsymbol{k}\cdot\boldsymbol{b}} \varphi_k$$

$$= \int \frac{\mathrm{d}z}{2\pi} \varphi(\boldsymbol{b}, z) \exp(-i\omega z/\gamma v), \tag{4}$$

where $\boldsymbol{k} = (\boldsymbol{k}_\perp, \omega/\gamma v)$ and φ_k is the Fourier component of the atomic potential which we define as

$$\varphi_k = \int \mathrm{d}^3 \boldsymbol{r}\, \mathrm{e}^{-i\boldsymbol{k}\cdot\boldsymbol{r}} \varphi(\boldsymbol{r}). \tag{5}$$

In the VP spectrum (4) the first term represents the contribution of the component of the electric field $E'_\perp$ which is perpendicular to the OZ axis, whereas the second term represents the contribution of the component $E'_\parallel$, which is parallel to the OZ axis in the rest frame. As a rule [22]), the second term contribution is ignored when $\gamma \gg 1$ because $E'_\parallel / E'_\perp \sim \gamma^{-1}$. As it is shown in ref. [21]), when calculating the EE or ED cross sections, the second term is responsible for the transitions with change of angular momentum projection $\Delta M = 0$. As one can prove, if one substitutes the Coulomb potential $\varphi(r) = Ze/r$ into eqs. (4) and (5), one obtains the standard VP spectrum from ref. [22]), p. 722. The first of the two representations of $\mathcal{J}(\omega, \boldsymbol{b})$ in eq. (4) is essentially convenient for the calculation of the VP spectrum in collisions with atoms, since φ_k is connected with the atomic form factor and is often approximated by simple expressions.

When the relativistic nucleus penetrates through the crystal parallel to an atomic string at a relatively small impact parameter $b < a$, fig. 1a, one need to take into account only the potential of the nearest string, which is defined by:

$$\varphi_N(\boldsymbol{r}) = \sum_{n=1}^{N} \varphi(\boldsymbol{r} - \boldsymbol{r}_n), \qquad \boldsymbol{r}_n = (\boldsymbol{b}, z_n), \tag{6}$$

where r_n is the coordinate of the nth atom and N is the number of atoms in the string. The Fourier component of the potential (6) is

$$\varphi_k^N = \varphi_k \sum_{n=1}^{N} e^{ik\cdot r_n}, \tag{7}$$

where φ_k is the Fourier component of the atomic potential (5). After substituting (7) into (4) and neglecting the second term in (4), and then averaging over possible deflections of the atoms in the chain due to the thermal vibrations (the procedure is similar to those used in the theory of neutron and X-ray diffraction and in the coherent bremsstrahlung theory, e.g. ref. [10])) one obtains the following formula for the VP-flux spectral density for the case when $\boldsymbol{v}$ is parallel to the atomic string:

$$\frac{dn_N(\omega, \boldsymbol{b})}{d\omega} = \frac{c}{\hbar\omega v^2}\left\{\left|\sum_{n=1}^{N} \exp\left(\frac{i\omega a n}{\gamma v}\right)\right|^2 I_2(\omega, \boldsymbol{b}) \exp\left[-\left(\frac{\omega\sigma}{\gamma v}\right)^2\right]\right.$$
$$\left. + N\left[I_1(\omega, \boldsymbol{b}) - I_2(\omega, \boldsymbol{b}) \exp\left(-\left(\frac{\omega\sigma}{\gamma v}\right)^2\right)\right]\right\}, \tag{8}$$

$$I_1(\omega, \boldsymbol{b}) = \int\int \frac{d^2\boldsymbol{k}_\perp}{(2\pi)^3} \cdot \frac{d^2\boldsymbol{k}'_-}{(2\pi)^3} (\boldsymbol{k}_- \boldsymbol{k}'_\perp) \varphi_k \varphi^*_{k'} \exp\left[i(\boldsymbol{k}_\perp - \boldsymbol{k}'_\perp)\boldsymbol{b} - \tfrac{1}{2}(\boldsymbol{k}_\perp - \boldsymbol{k}'_-)^2\sigma^2\right], \tag{9}$$

$$I_2(\omega, \boldsymbol{b}) = \left|\int \frac{d^2\boldsymbol{k}_\perp}{(2\pi)^3} \boldsymbol{k}_\perp \varphi_k \exp\left[i\boldsymbol{k}_\perp \boldsymbol{b} - \tfrac{1}{2}\boldsymbol{k}_-^2\sigma^2\right]\right|^2, \tag{10}$$

$$\boldsymbol{k}^2 = \boldsymbol{k}_-^2 + (\omega/\gamma v)^2, \qquad (\boldsymbol{k}')^2 = (\boldsymbol{k}'_-)^2 + (\omega/\gamma v)^2, \tag{11}$$

where σ^2 is the mean-square amplitude of uncorrelated thermal vibrations of atoms.

After integrating over all impact parameters b, which corresponds to the assumption of a uniform particle flux, and after performing the n-summation, the following more simple expression appears:

$$\frac{dn_N(\omega)}{d\omega} = \frac{c}{\hbar\omega v^2}\left\{I_2(\omega)\frac{\sin^2(\omega a N/2\gamma v)}{\sin^2(\omega a/2\gamma v)} \exp\left[-\left(\frac{\omega\sigma}{\gamma v}\right)^2\right]\right.$$
$$\left. + N\left[I_1(\omega) - I_2(\omega)\exp\left[-\left(\frac{\omega\sigma}{\gamma v}\right)^2\right]\right]\right\},$$
$$I_1(\omega) = \int \frac{d^2\boldsymbol{k}_-}{(2\pi)^4} \boldsymbol{k}_-^2 |\varphi_k|^2,$$
$$I_2(\omega) = \int \frac{d^2\boldsymbol{k}_\perp}{(2\pi)^4} \boldsymbol{k}_\perp^2 |\varphi_k|^2 e^{-\boldsymbol{k}_\perp^2\sigma^2}. \tag{12}$$

It should be mentioned that $I_1(\omega)$ contains a logarithmic divergence since $\varphi_k \sim k^{-2}$ for $k \to \infty$ (Coulomb at small distances) and one should use $k_{max} \sim R_{nucl}^{-1}$ according to the VP method. The closer collisions contribute to the EE process too, but cannot be distinguished from the usual nuclear reactions [2]).

The VP spectrum (eqs. (8) and (12)) affecting the nuclei during the motion parallel to the atomic chain in the crystal has sharp maxima at the frequencies $\omega_n = (2\pi\gamma v/a)n$, $n = 1, 2, \ldots$, which are proportional to the frequency of transit between neighbouring string atoms in the nucleus rest frame, see fig. 2. When $\omega = \omega_n$, the VP spectrum $dn_N(\omega)/d\omega$ is proportional to the square of the number of atoms along the straight-line part of the nuclear trajectory near the string. The region between the nth and $(n+1)$th basic maxima includes $N-2$ lower maxima. The width of the basic Γ_N and the lateral Γ_n maxima are: $\Gamma_N = 2\Gamma_n \approx \omega_1/N$. With fixed γ and $N \gg 1$ we have $\Gamma_N \to 0$ and the coherent part of the VP spectrum (eqs. (8) and (12)) becomes a sum of delta-functions like $\delta(\omega - \omega_n)$. With fixed N and increasing γ the width of the basic and lateral maxima increases and can exceed the nuclear level width Γ. The relation between $\Gamma_N = \Gamma_N(N, \gamma)$ and Γ appears to be very important in analysis of coherent relativistic EE (see sect. 3, below).

Note, that the VP spectra (eqs. (8) and (12)), similar to other cross sections connected with the particle-crystal interaction, e.g. ref. [10]), include a coherent part proportional to $|\sum_n \exp(i\omega an/\gamma v)|^2$ and an incoherent one. The incoherent part is

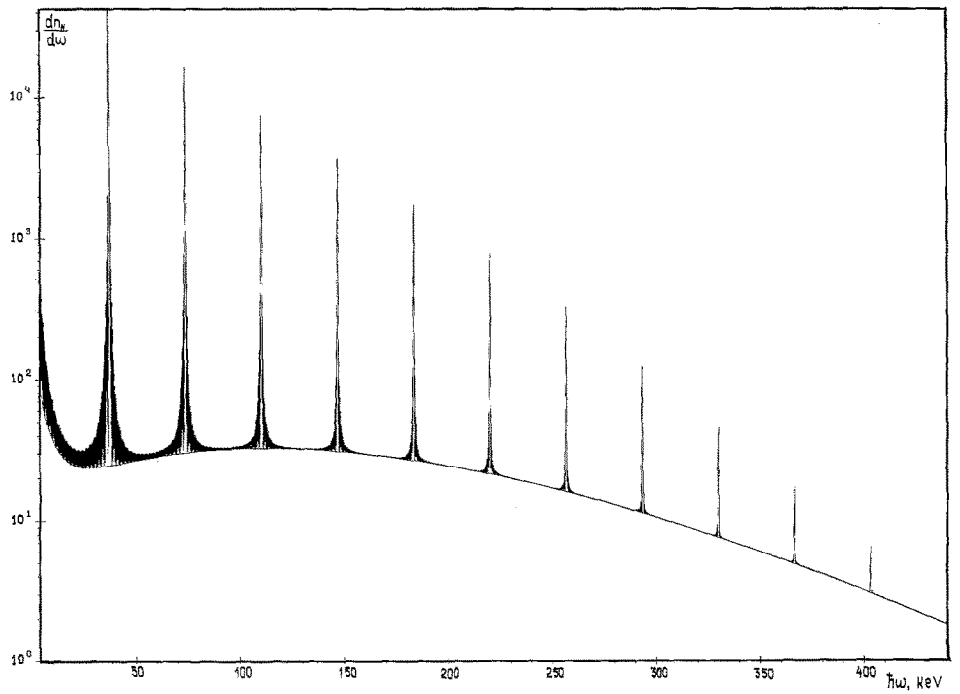

Fig. 2. The VP spectrum effecting the nuclei under axial motion parallel to the ⟨110⟩ atomic string in the gold crystal, calculated according to eq. (15). The crystal temperature $T = 293$ K and $a_z = 2.8 \times 10^{-8}$ cm. For the γ-value chosen the position of the third harmonic in the spectrum coincides with the transition energy $\hbar\omega_0 = 110$ keV between the lowest levels of the ^{19}F nucleus, i.e. the equality $\omega_0 = 2\pi\gamma vn/a_z$ with $n = 3$ ($\gamma = 8.467$) takes place.

proportional to the number N of atoms and disappears for $\sigma^2 \to 0$ in (12) or for $b > \sigma$ or for $\gamma \gg 1$ in (12). At the same time the obtained VP spectrum (8) of an atomic string shows a new peculiarity in comparison with the VP spectrum (4) of the individual atom. That is, the absence of divergence of the coherent part in (8) at $b \to 0$ for the atomic potential with the screening of Moliere type, as compared to (4) (for details see ref. [17])). The physical reason for this behaviour lies in the fact that the mean-square displacement of atoms in the string from the OZ axis does not equal zero, but equals the mean-square amplitude of thermal vibrations of atoms in the crystal. Therefore, the coherent part of VP spectrum is maximal for the nuclei passing at the distance $b \approx \sigma$ from the atomic string. The incoherent part of the VP spectrum (8), due to the presence of $I_1(\omega, \boldsymbol{b})$ has the divergence even for the Moliere atomic potential at $b \to 0$. The distances $b \approx \sigma$ are thus most important for the resonant EE of relativistic nuclei. The coherent part of the VP spectrum exceeds by approximately N times the incoherent one at $b \approx \sigma$, if $\omega = \omega_n$ and $n < 10$ (see fig. 2).

3. Energy dependence of the EE probability in a crystal

When the VP spectrum is known, the probability of the electric dipole EE is found immediately (see, e.g. ref. [21])):

$$P_{\mathrm{if}}^{N}(\boldsymbol{b}) = \int \mathrm{d}\omega \frac{\mathrm{d}n_N(\omega, \boldsymbol{b})}{\mathrm{d}\omega} \frac{16\pi^3}{9} \frac{\omega}{\hbar c} B(\mathrm{E1}) \rho_{\mathrm{f}}(\omega) , \tag{13}$$

where $B(\mathrm{E1})$ is the standard reduced probability of the electric dipole transition between the nuclear levels (see e.g. ref. [1])) and $\rho_{\mathrm{f}}(\omega)$ is the density of final states. The cross section of EE follows from (13) after integration over impact parameters b. The resonant excitation of the nuclear low-lying levels by means of the specific VP spectrum $\mathrm{d}n_N/\mathrm{d}\omega$, with its sharp maxima at $\omega = \omega_n$ (see fig. 2), is of great interest. In this case one should make the replacement [see, e.g. ref. [1]), p. 41]

$$\rho_{\mathrm{f}}(\omega)\, \mathrm{d}\omega \to \frac{1}{2\pi} \frac{\Gamma}{[(\omega - \omega_0)^2 + \frac{1}{4}\Gamma^2]} \mathrm{d}\omega , \tag{14}$$

where ω_0 is the resonant transition frequency between two nuclear levels and Γ is the full width of the excited level. With

$$\frac{16\pi}{9} \left(\frac{\omega_0}{c}\right)^3 B(\mathrm{E1}) = g\hbar\Gamma_\gamma , \qquad g = \frac{2I_{\mathrm{f}} + 1}{2I_{\mathrm{i}} + 1} , \tag{15}$$

where $\hbar\Gamma_\gamma$ is the radiation width of the excited level, and considering $\Gamma \approx \Gamma_\gamma$ we obtain for the EE probability in the crystal the following formula:

$$P_{\mathrm{if}}^{N}(\boldsymbol{b}, \gamma) = \int \frac{\mathrm{d}n_N(\omega, \boldsymbol{b})}{\mathrm{d}\omega} g \frac{\pi}{2} \left(\frac{c}{\omega}\right)^2 \frac{\Gamma_\gamma^2}{[(\omega - \omega_0)^2 + \frac{1}{4}\Gamma_\gamma^2]} \mathrm{d}\omega . \tag{16}$$

Here the shape of the VP spectrum $dn_N/d\omega$, e.g. the maxima positions, depends on the nucleus Lorentz-factor γ. By changing γ one can try to get a coincidence of ω_n and ω_0. This case corresponds (see below) to the coherent addition of the excitation amplitudes from the various atoms of the string in a crystal with the corresponding phase shifts being a multiple of 2π.

In any experiment a real nuclear beam has a certain energy spread $\Delta\gamma$. If the VP spectrum is calculated for a definite γ-value corresponding to the centre of the distribution over γ, a distribution of the nuclei over the velocities v_z' occurs in the primed (rest) frame. This results [17]) in a Doppler broadening of the VP absorption cross section by the nuclei, which can be taken into account by substituting in (16) Γ_D for Γ and $\Gamma_\gamma\Gamma_D$ for Γ_γ^2. The Doppler width for this case is defined [17]) by

$$\Gamma_D \approx \Gamma_\gamma + \omega_0 \frac{\Delta v_z'}{c} \approx \Gamma_\gamma + \omega_0 \frac{c}{v}\frac{\Delta\gamma}{\gamma}, \tag{17}$$

As a rule, $\Delta\gamma/\gamma \approx 10^{-3}$ and $\Gamma_D \gg \Gamma_\gamma$. Another way to take into account the energy spread in the incident nuclear beam is discussed in ref. [23]).

To analyze the energy dependence of the relativistic coherent EE in a relatively thin crystal, where the nuclear flux is uniform, it is convenient to introduce the dimensionless ratio

$$R(\gamma) = \frac{\int d^2\boldsymbol{b}\, P_{if}^N(\boldsymbol{b}, \gamma)}{N\int d^2\boldsymbol{b}\, P_{if}^1(\boldsymbol{b}, \gamma)} = \frac{\sigma_N(\gamma)}{N\sigma_1(\gamma)}. \tag{18}$$

Here the denominator represents the EE cross section in nuclear collisions with N separate atoms. For the estimations it is convenient to use the Doyle-Turner atomic form factors [24])

$$\varphi_k = \sum_{i=1}^{4} a_i \exp(-b_i \boldsymbol{k}^2), \tag{19}$$

with the constants a_i, b_i tabulated for various crystals. It should be stressed that (19) is unphysical at large k-values and this decreases the contribution of small impact parameters to the incoherent rate. Further, since in this case no divergence appears during integration over $\boldsymbol{b}$, we can integrate over all impact parameters. This simple model (a more realistic estimation is given below, compare eq. (33)) leads to the simple final expression for $R(\gamma)$, when $\Gamma_N \gg \Gamma_D$:

$$R(\gamma) = \frac{I_2(\omega_0)}{NI_1(\omega_0)}\left|\sum_{n=1}^{N} \exp(i\omega_0 na/\gamma v)\right|^2 \exp[-(\omega_0\sigma/\gamma v)^2] + \left[1 - \frac{I_2(\omega_0)}{I_1(\omega_0)}\exp[-(\omega_0\sigma/\gamma v)^2]\right], \tag{20}$$

where $I_1(\omega_0)$, $I_2(\omega_0)$ are the same as in eq. (12). In the opposite case, $\Gamma_N \leqslant \Gamma_D$, numerical integration over ω should be done in the formula (16). Fig. 3a shows

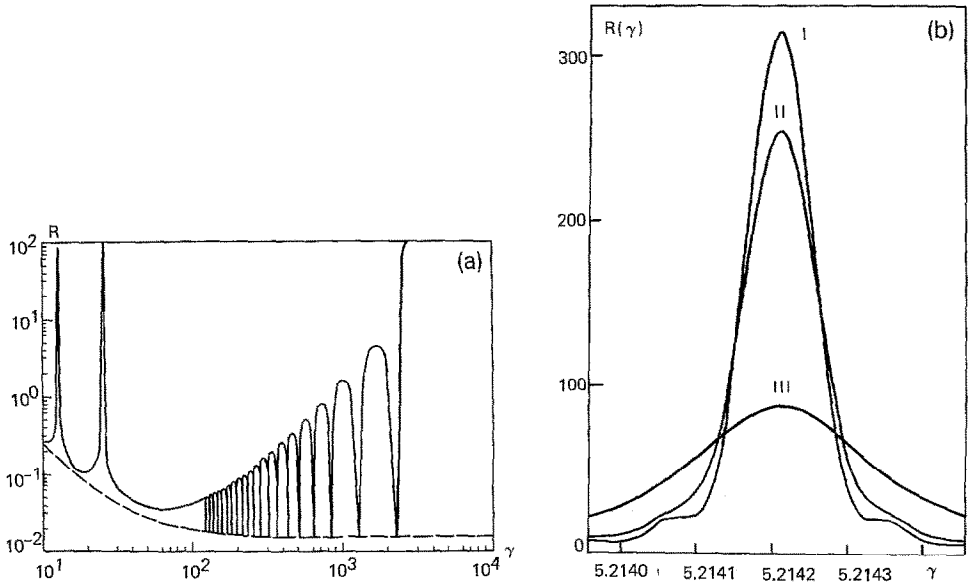

Fig. 3. The $R(\gamma)$ dependence for $N = 10^2$ in the wide γ-region (a) and near the resonance with $n = 5$ ($\gamma = 5.2142$) for $N = 10^3$ (b) and for different energy spread in the nuclei beam: I - $\Delta\gamma/\gamma = 10^{-5}$, II - $\Delta\gamma/\gamma = 10^{-4}$, III - $\Delta\gamma/\gamma = 10^{-3}$. Both figures are given for ^{19}F nucleus and ⟨110⟩ Au axis, $T = 293$ K. The dashed line in (a) represents incoherent background.

that for the EE of 110 KeV of ^{19}F nucleus (E1 electric dipole transition). Two specific regions are clearly seen: the region of resonances at $\gamma < 10^2$ and the region of increasing oscillations at $\gamma \gg 10^2$. The behaviour of $R(\gamma)$ near one of the resonances is shown in fig. 3b; where the resonances are the results of the numerical integration over ω in eq. (16). Similar results, but without taking into account the γ spread, were obtained earlier in ref. [19]). Thus, the energy spread of the nuclear beam influences significantly the magnitude and the width of the resonance in the EE of nuclei passing through the crystals.

Let us consider the space-time interpretation of the development of the EE process in the crystal, following ref. [19]). According to the VP method, resonances in the coherent EE of relativistic nuclei under axial channeling take place when $\omega_0 = (2\pi\gamma v/a)n$, i.e. when the transition frequency between two nuclear levels is a multiple of the transit frequency between two atoms in the string, calculated in the rest frame of the nucleus, or coincides with the position of the nth maximum in the VP spectrum in the crystal. On the other hand, as one can see from eqs. (8) and (12) the interferential multiplier $\exp(in\omega_0 a/\gamma v)$ results due to addition of the same amplitudes with the different phases $\Delta_n = n\Delta = n(\omega_0 a/\gamma v)$. The resonant condition means, from this point of view, $\Delta = 2\pi k (k = 0, 1, 2, \ldots)$. In this case the region of sharp resonances in fig. 3a corresponds to $\Delta = 2\pi k$ with $k \geq 1$. For the case $\gamma \gg 1$ we obtain $\Delta \to 0$ and that means, the phase shift between any two neighbouring exponents is

negligible:

$$\Delta = \frac{\omega_0 a}{\gamma v} = \omega_0 \tau \ll 2\pi . \tag{21}$$

Here τ is the transit time between two neighbouring atoms of the string, calculated in the rest frame of the nucleus. The inequality (21) corresponds to partial (incomplete) coherence. If the phase shifts between all N exponents in eqs. (8), (12) are negligible, i.e.

$$N\Delta = N\omega_0 \tau \ll 2\pi , \tag{22}$$

or

$$\gamma > \gamma_{\text{ass}} = \frac{N}{2\pi} \frac{\omega_0 a}{v} , \tag{23}$$

then all amplitudes of EE are added coherently and we are in the limit of full (complete) coherence. In this case the amplitude of EE under axial channeling is proportional to the number N of atoms in the string, the cross section increases and $R(\gamma) \to N$, if $\gamma \gg 1$.

After introducing $t = Na/v$ - the transit time through the crystal, calculated in the laboratory frame, and the characteristic "intrinsic" nuclear time $T = 2\pi/\omega_0$, the inequality (23) can be rewritten in the form:

$$\gamma T > t . \tag{24}$$

The inequality (24) means, that when the time of the development of the process of nuclear EE, γT, exceeds the transit time t through the crystal, the amplitudes of EE resulting due to interaction with all N atoms of the crystal string are added in phase, or coherently (here, we do not take into account any damping processes during the transit time). After multiplying eq. (24) by v, it can be rewritten in the form:

$$L_{\text{ex}} = \gamma v T > L = Na , \tag{25}$$

where L_{ex} means the length of the development of the nuclear EE and $L = Na$ is the string length. Thus, if the length L_{ex} of the development of EE exceeds the length of the atomic string L, the cross section of this process is proportional to the square of the number of atoms in the string. When L_{ex} greatly exceeds L, the order of arrangement of the atoms along the OZ axis is not important.

Let us qualitatively consider the energy dependence of coherent EE by means of the VP method. Fig. 4 represents the VP spectra corresponding to various γ-values. Fig. 4a corresponds to the case of resonance for EE of the 110 KeV level of the ^{19}F nucleus at $\gamma_1 = 25.4$, when the first-order maximum in the VP spectrum coincides with the position of the maximum in the photoabsorption cross section ω_0. In this case the EE cross section is defined by integration over ω of $\sigma(\omega)$, multiplied by $dn_N/d\omega$ and is obviously proportional to N^2. Fig. 4b represents the nonresonant case with $\omega_1 = 2\pi\gamma_2 v/a \gg \omega_0$, $\gamma_2 \gg \gamma_1$. This kind of VP spectrum results in a $R(\gamma)$ dependence like that given in fig. 3a for γ-values $\sim 10^2 - 10^3$. Fig. 4c shows that

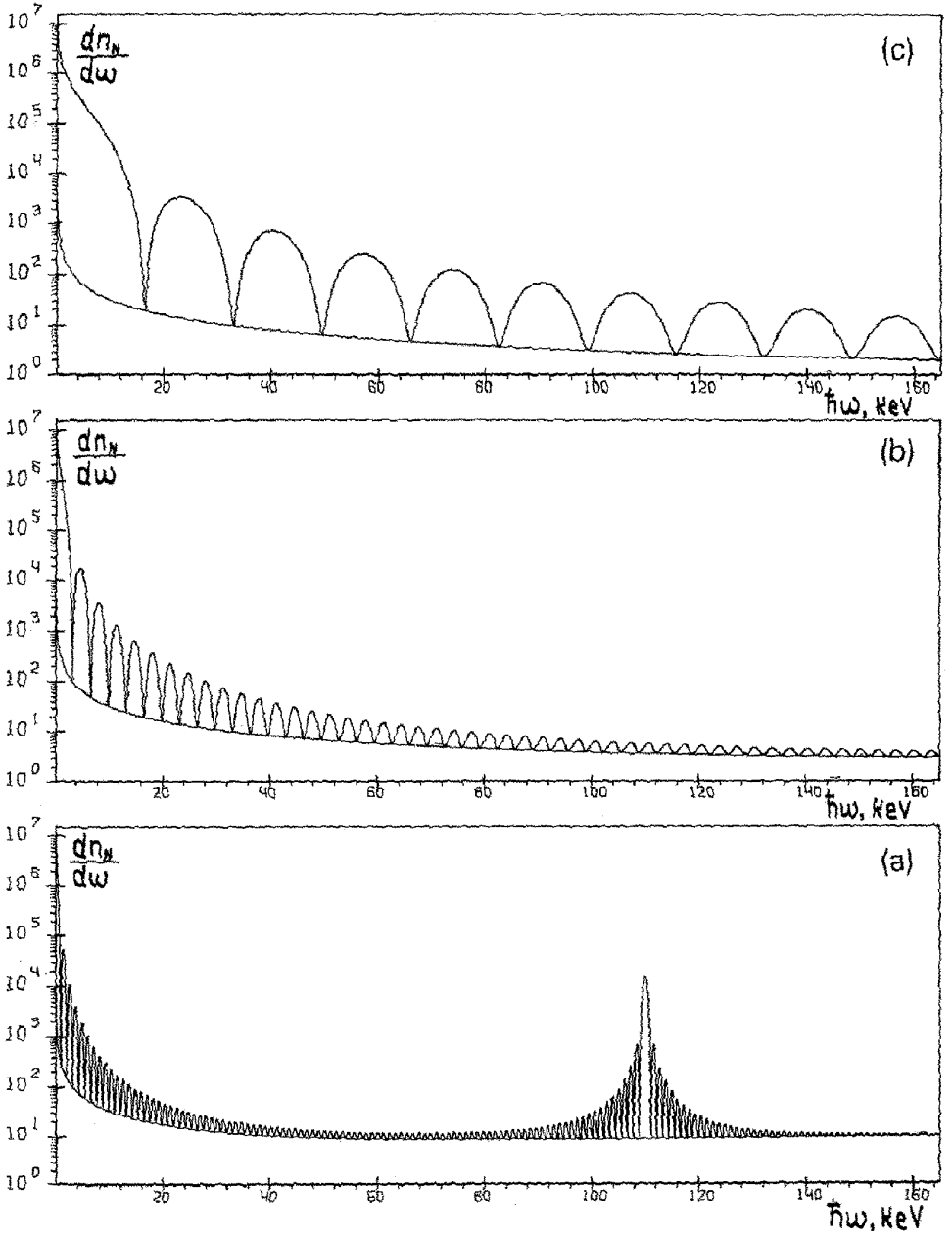

Fig. 4. Interpretation of the resonances and high-energy increasing of the EE cross section in the frame of the VP method ($\langle 110\rangle$ Au, $N = 10^3$): (a) one of the peaks in the VP spectrum coincides at $\gamma = \gamma_1$ with the position of the maximum in the photon resonant absorption cross section (the case of 110 keV level of the ^{19}F nucleus); (b) the region without resonances at $\gamma > \gamma_1$; (c) the region $\gamma \gg \gamma_1$ and the beginning of the increase of the EE cross section. Here a "zero-order" harmonic width is comparable with the $\hbar\omega_0 = 110$ keV value.

with further increasing γ value ($\gamma_3 \gg \gamma_2$) the VP spectrum near $\omega = \omega_0$ is determined by the vicinity of the "zero-order" maximum. The width of this "zero-order" maximum, $\Gamma_N = 2\pi\gamma v/aN$, can exceed ω_0 and in this case the EE cross section is proportional to N^2. The region of γ-values where $L_{ex} > L$ is not connected with any resonances and is called the region of complete coherence. Thus, for $L_{ex} > L$ the full EE cross section of relativistic nuclei passing through thin crystals is proportional to $\sigma_1 N_\perp N^2$, where $N_\perp$ is the number of the strings, with which the nuclei interacted, and N is the number of atoms along the straight-line path of the nucleus near these strings.

For quantitative comparison of the relativistic EE in crystals with that in an amorphous target one should calculate the VP spectrum (4) integrated over impact parameters $b > R_{min}$, with R_{min} being the sum of the radii of the colliding nuclei. For such small b-values one should use a Moliere-type form factor instead of the Doyle-Turner (eq. (19)):

$$\varphi_k = \sum_{i=1}^{3} \frac{4\pi\alpha_i Ze}{k^2 + \kappa_i^2}, \qquad \alpha_i = \{0.1; 0.55; 0.35\}, \quad \kappa_i = \kappa\{6.0; 1.2; 0.3\}, \tag{26}$$

where κ^{-1} is the Thomas-Fermi screening radius.

Further, when $\gamma \gg 1$, one can neglect the longitudinal terms in the VP spectrum and obtain

$$\frac{dn^M}{d\omega}(\omega, \boldsymbol{b}) = \frac{\alpha Z^2}{\omega\pi^2}\left(\frac{c}{v}\right)^2 \left| \sum_{i=1}^{3} \alpha_i \kappa_\omega^i K_1(\kappa_\omega^i b) \right|^2,$$

$$(\kappa_\omega^i)^2 = \kappa_i^2 + (\omega/\gamma v)^2, \qquad \alpha = e^2/\hbar c, \tag{27}$$

where $K_1(x)$ is a McDonald function. The integration of (27) over $b > R_{min}$ results in

$$\frac{dn^M}{d\omega}(\omega) = \frac{2\alpha Z^2}{\pi\omega}\left(\frac{c}{v}\right)^2 \sum_{i,j=1}^{3} \alpha_i\alpha_j\xi_i\xi_j \times \left\{ (1-\delta_{ij}) \frac{\xi_i K_0(\xi_i)K_1(\xi_j) - \xi_j K_0(\xi_j)K_1(\xi_i)}{\xi_i^2 - \xi_j^2} + \tfrac{1}{2}\delta_{ij}\left[\frac{2}{\xi_i} K_0(\xi_i)K_1(\xi_i) - (K_1^2(\xi_i) - K_0^2(\xi_i)) \right] \right\}, \tag{28}$$

where $\xi_i = \kappa_\omega^i R_{min}$ and the EE cross section in a nuclear collision with a separate atom has the form

$$\sigma_1^M(\gamma, R_{min}) = \int d\omega \frac{dn^M}{d\omega}(\omega)\, g \frac{\pi}{2}\left(\frac{c}{\omega}\right)^2 \frac{\Gamma_\gamma \Gamma_D}{[(\omega-\omega_0)^2 + \frac{1}{4}\Gamma_D^2]}. \tag{29}$$

From the formula (29), in the limit of very sharp resonance in the photoabsorption cross section, it follows that

$$\sigma_1^M(\gamma, R_{min}) \approx g\pi^2\left(\frac{c}{\omega_0}\right)^2 \Gamma_\gamma \frac{dn^M}{d\omega}(\omega_0). \tag{30}$$

For the estimation of $\sigma_1^{M1}(\gamma, R_{min})$ one can use the approximate formula

$$\sigma_1^{M}(\gamma, R_{min}) \approx \left(\frac{Z_1 e^2}{\hbar c}\right)^2 \frac{B(\mathrm{E1}, I_i \to I_f)}{e^2} \frac{32\pi^2}{9} \left(\frac{c}{v}\right)^2 \ln\left(\frac{C}{\xi_\kappa}\right), \tag{31}$$

which follows from eqs. (28), (30), if we take $\xi_i = \xi_j = \kappa_\omega R_{min} = \xi_\kappa$ and consider $\xi_\kappa \ll 1$ (where $C = 0.681085$). If we put $\kappa = 0$, we obtain the approximate formula for relativistic dipole excitation, given by Winther and Alder [ref. [2]), formula (1.15)] for the case of nuclear collisions with the nonscreened Coulomb potential at $\gamma \gg 1$. Since for the typical resonant gamma values ($\gamma \leqslant 20$) we have $\xi_\kappa \geqslant 1$, it is necessary to use the exact formulae (28), (30) for the calculation of $\sigma_1(\gamma, R_{min})$. Using these formulae and $\kappa_i = \kappa_j = \kappa$ one can compare for example, the cross sections with $b > R_{min}$ and with $b > R'_{min}$ calculating $F(\gamma) = \sigma_1(\gamma, R'_{min})/\sigma_1(\gamma, R_{min})$:

$$F(\gamma) = \frac{K_0(x)K_1(x) - \frac{1}{2}x(K_1^2(x) - K_0^2(x))}{K_0(y)K_1(y) - \frac{1}{2}y(K_1^2(y) - K_0^2(y))},$$

$$x = \kappa_\omega R'_{min}, \qquad y = \kappa_\omega R_{min}. \tag{32}$$

Fig. 5 presents $F(\gamma)$ values for the concrete case of the E1 transition in $^{19}F(\hbar\omega_0 = 110\ \mathrm{KeV})$, interacting with Au atom, for different R'_{min} values. This result shows the relative contribution of distant collisions to the EE cross section in this γ-region.

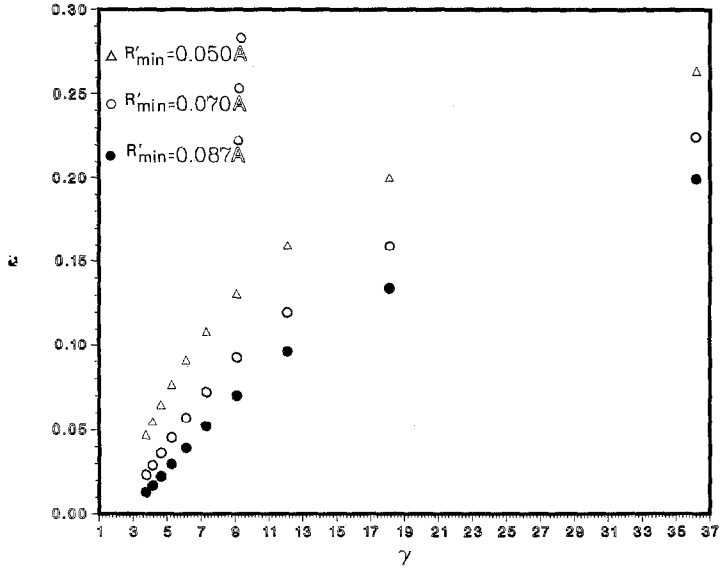

Fig. 5. The $F(\gamma)$ dependence for the case of excitation of the 110 keV level of a nucleus in collision with Au atom ($\kappa^{-1} = 0.109 \times 10^{-3}$ cm, $Z = 79$) for different R'_{min} values. The $F(\gamma)$ values are calculated for the first 10 resonant γ-values in the (110) direction in the Au crystal. The R'_{min} values used correspond to the mean-square amplitude σ of thermal vibration of the Au atom at the target temperatures $T = 100$ K, 200 K and 293 K, respectively.

Using eqs. (28), (30), one can estimate more accurately, in comparison with eq. (20), the relative value of the effect of resonant coherent EE under axial alignment as

$$\frac{\sigma_N(\gamma)}{N\sigma_1^{\mathrm{M}}(\gamma, R_{\min})} \approx R(\gamma)\frac{\sigma_1^{\mathrm{DT}}(\gamma)}{\sigma_1^{\mathrm{M}}(\gamma, R_{\min})} = R(\gamma)\frac{\mathrm{d}n_1^{\mathrm{DT}}(\omega)}{\mathrm{d}n_1^{\mathrm{M}}(\omega)}, \tag{33}$$

where $\mathrm{d}n_1^{\mathrm{DT}}(\omega)$, $\mathrm{d}n_1^{\mathrm{M}}(\omega)$ are defined by formula (12) for the Doyle-Turner and by formula (28) for the Moliere atomic form-factors, respectively, and $R(\gamma)$ is the same as in eq. (20). Since

$$\frac{\mathrm{d}n_1^{\mathrm{DT}}}{\mathrm{d}\omega}(\omega) = \frac{c}{\hbar\omega v^2} I_1^{\mathrm{DT}}(\omega), \tag{34}$$

$$I_1^{\mathrm{DT}}(\omega) = \frac{1}{(2\pi)^4}\sum_{i,j=1}^{4} \pi a_i a_j \frac{\exp\left[-(b_i+b_j)(\omega/\gamma v)^2\right]}{(b_i+b_j)^2}, \tag{35}$$

using this result, we guess:

$$\frac{\sigma_N(\gamma)}{N\sigma_1^{\mathrm{M}}(\gamma, R_{\min})} \approx R(\gamma)(5\times 10^{-2}-2\times 10^{-1}), \qquad 3 \leqslant \gamma \leqslant 25. \tag{36}$$

At the resonance ($\omega_0 = \omega_n$) we have $R(\gamma) \approx N$, but this relation is very sensitive to the N and $\Delta\gamma$ values, see fig. 3. Thus at the resonant condition $\omega_n = \omega_0$ (or for $\gamma > \gamma_{\mathrm{ass}}$) the relativistic EE cross section in the crystal can exceed sufficiently the EE cross section in an amorphous target, if the number N of atoms along the straight-line path of the nuclei near the separate atomic string is enough large. The number N is estimated usually as $N \simeq \kappa^{-1}/\psi_{\mathrm{L}} a$ where ψ_{L} is the Lindhard's critical angle [8]) and κ^{-1} is the screening radius. Really, the N-value for the resonant γ-values can reach $N \approx 10^2$–10^3 and increases $\sim\sqrt{\gamma}$ with increasing nuclear energy in the region of complete coherence, $\gamma > \gamma_{\mathrm{ass}}$.

In conclusion to this section, we note, that the relativistic EE under axial channeling conditions in the crystals leads, in the case of resonance to high probability for E1 dipole transitions with nuclear momentum projection change $\Delta M = \pm 1$ (the transition probability with $\Delta M = 0$ is negligible for $\gamma \gg 1$). This phenomenon can be investigated experimentally at the modern relativistic heavy-ion accelerators.

4. Energy dependence of relativistic deuteron ED in crystals

Electromagnetic disintegration (ED) is another process which results during the interaction of relativistic nuclei with the target atoms. ED is possible both for relativistic projectile nuclei and the target nuclei. Below we consider only the ED of the projectile nuclei.

Similar to the case of coherent EE under axial alignment in the crystals, the cross section of coherent ED is calculated by means of the VP method. Let $\gamma \gg 1$, then the "longitudinal" part of the VP spectrum is negligible and

$$\frac{\mathrm{d}\sigma_{\mathrm{d}}}{\mathrm{d}\Omega}(\gamma) = \int \mathrm{d}^2\boldsymbol{b} \int \frac{\mathrm{d}n_{\mathrm{N}}(\omega, \boldsymbol{b})}{\mathrm{d}\omega}\frac{16\pi^3}{9}\frac{\omega}{\hbar c} B(\mathrm{E1}, \omega, \Omega)\rho_{\mathrm{f}}(\omega)\,\mathrm{d}\omega. \tag{37}$$

Here, $\rho_f(\omega)$ is the final states density and we suppose that for qualitative analysis it is enough to use $dn_N(\omega, \boldsymbol{b})/d\omega$ calculated with the Doyle-Turner form factors (19) and integrate over all impact parameters. For the deuteron nucleus the E1 transition is dominant and the $B(E1, \omega, \Omega)$ function is well known [25]. After using the $B(E1, \omega, \Omega)$ value in the zero-range approximation from ref. [25]) and integration over emission angles one obtains

$$\sigma_d(\gamma) = \int d^2\boldsymbol{b} \int \frac{dn_N(\omega, \boldsymbol{b})}{d\omega} \sigma_{E1}(\omega)\, d\omega, \tag{38}$$

$$\sigma_{E1}(\omega) = \frac{8\pi\alpha}{3} \frac{\hbar^2}{m} \frac{\sqrt{\varepsilon}\,(\hbar\omega - \varepsilon)^{3/2}}{(\hbar\omega)^3}, \tag{39}$$

where α is the fine structure constant, $\varepsilon = 2.223$ MeV is the deuteron binding energy and m is the nucleon mass. The results of the numerical calculations with the use of formulae (38) and (39) are given in figs. 6 and 7. The specific behaviour of $\sigma_d(\gamma)$ is explained as follows. The coherent part of the VP spectrum (eq. (8) or (12)) consists approximately of ten harmonics (or basic maxima, see fig. 2), since the other ones are suppressed due to the "thermal" exponent, $\exp[-(\omega_n\sigma/\gamma v)^2]$. This part of the VP spectrum, arranged in the region $\Delta\omega$, shifts linearly with the γ-value increasing. At $\gamma < 10^2$ and $\gamma > 10^3$ this region lies far away from the region where the photodisintegration cross section $\sigma_{E1}(\omega)$ is more effective, and that leads to the decreasing of $\sigma_d(\gamma)$ at those γ-values, see fig. 5. When $\gamma \gg 10^3$, the effects of incomplete coherence occur, like in the coherent EE (cf., e.g. with fig. 3a). That occurs when

$$\Delta_d = \frac{\varepsilon}{\hbar} \frac{a}{\gamma v} \ll 1, \tag{40}$$

i.e. when the phase shift between ED amplitudes from two neighbouring atoms in the string becomes small and that leads to the increase of the ED cross section, fig. 6b. Finally, at

$$\gamma > \gamma_{coh} = a(\varepsilon N/2\pi\hbar v) \approx 10^3 N, \tag{41}$$

the regime of complete coherence takes place. That means, all N amplitudes of ED from the atoms of the string are summing in the phase and $\sigma_d(\gamma)$ becomes proportional to N^2, fig. 6b. From the point of view of the VP method, the conditions (40)-(41) mean that the effective region of the $\sigma_{E1}(\omega)$ is reached by the vicinity of the "zero-order" maximum in the VP spectrum of the string, with the width of the "zero-order" maximum $\Gamma_N = 2\pi\gamma v/aN$. From the other point of view, the conditions (40)-(41) correspond, as in the case of the coherent EE (see, sect. 3), to the case when the length of the development of the process, $L_{ex} \approx 2\pi\gamma\hbar v/\varepsilon$ exceeds greatly the atomic string length, $L = Na$. It is essential to note, that even at $L_{ex} > a$ the small longitudinal (parallel to the OZ direction) thermal vibrations of the atoms in the crystal are negligible, because they lead to the additional small phase shifts between

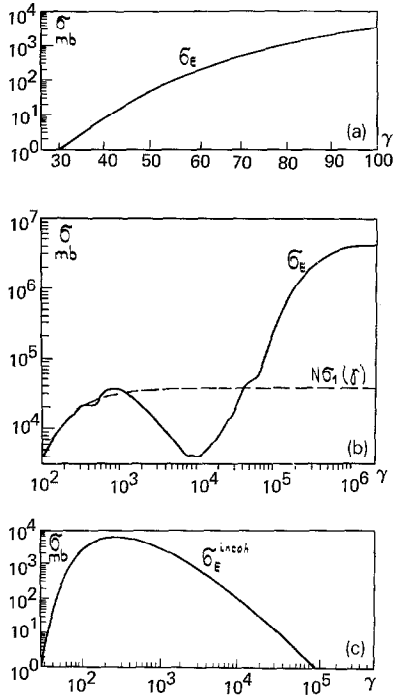

Fig. 6. The energy dependence (a), (b) of the coherent ED cross section of the deuterons in the crystal. Only E1 dipole electric transition is taken into account. Part (c) represents the behaviour of the incoherent part of the cross section. The dotted line is the ED cross section in the amorphous target with the same number of atoms. Calculations are provided for ⟨110⟩ Au axis for $T = 293$ K and $N = 10^2$, using the Doyle-Turner approximation of the atomic form factor.

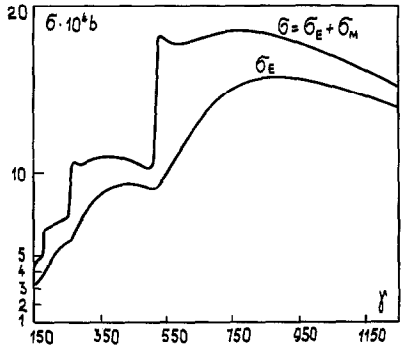

Fig. 7. A more detailed behaviour of the coherent ED cross section of deuterons in the crystal in the definite energy range. The upper curve represents the total cross section as the sum of the E1 and M1 transitions and the lower one shows the E1 transition only. The interference effects are clearly seen. The parameters are the same as in fig. 6.

amplitudes. As a consequence, the incoherent part of the ED cross section rapidly decreases with the γ-value increasing. What is more, at $L_{ex} \gg L$ the order of arrangement of the atoms along OZ axis is not so very important, similar to the EE in crystals (see sect. 3). This region of γ-values is not yet reached at the modern accelerators (e.g. for relativistic heavy ions in CERN $\gamma_{max} = 2 \times 10^2$). In principle, one could expect similar effects in the ionization cross section of relativistic ions containing several electrons and passing through thin crystals.

5. Computer simulation of the resonant EE in crystals

The theory of coherent EE of relativistic nuclei under axial channeling in a crystal, developed in sect. 3, is valid for the interaction with a separate atomic string, or for the interaction with thin crystals. To estimate the EE probability for the nuclei passing through rather thick crystals, it is enough to add incoherently the amplitudes from the different strings, as was done in ref. [23]). But to calculate this probability more accurately, it is necessary to take into account the bending of the real trajectories of the nuclei in crystals. The difference between the straight-line trajectories and the real ones should effect the magnitude of the resonances predicted by the theory, see fig. 3. Below we give the new method of the analysis of this phenomenon based on the computer simulation of the nuclear trajectories in a crystal together with the calculation of EE probabilities for the simulated trajectories.

The nuclear trajectories in the crystal are determined by way of the standard binary collision model [26]) which was successfully used recently in the computer simulation of the spectral and polarization characteristics of channeling radiation [27]). According to this model the scattering angle in the collision with the separate atom is calculated using the impulse approximation. The nuclear velocity changes instantaneously from $\boldsymbol{v}_k$ to $\boldsymbol{v}_{k+1}$ after the kth collision and remains constant between the collisions during the time $\Delta\tau_k = \tau_{k+1} - \tau_k$. Thermal vibrations of the crystal atoms are taken into account by choosing the atomic coordinates according to the normal distribution relative to the equilibrium. The energy losses in the target are not taken into account here and E1 dipole transition is considered.

When the nuclear trajectory is defined, the amplitude of the E1 dipole transition of the nucleus from the ground state to the excited one is determined by means of perturbation theory (cf., e.g. ref. [2])):

$$
\begin{aligned}
a_{if} &= \sum_{n=1}^{N} a_{if}^n = \sum_{n=1}^{N} \frac{1}{i\hbar} \sum_{\mu=-1}^{1} \sqrt{\tfrac{4}{3}\pi}\,(-1)^{\mu} \beta_{\mu}^n \langle f|\mathcal{M}(E1-\mu)|i\rangle\,, \\
\beta_{\mu}^n &= \boldsymbol{e}_{\mu} \cdot \frac{\partial}{\partial \boldsymbol{\rho}} \int_{\tau_n}^{\tau_{n+1}} dt\, e^{i\omega t} \gamma \varphi(\boldsymbol{r}(t))\,, \qquad \mu = \pm 1 \\
\beta_0^n &= -\frac{i\omega}{v\gamma^2} \int_{\tau_n}^{\tau_{n+1}} dt\, e^{i\omega t} \gamma \varphi(\boldsymbol{r}(t))\,, \\
\boldsymbol{r}^2(t) &= \boldsymbol{\rho}_n^2 + \gamma^2 v_n^2 t^2\,.
\end{aligned}
\tag{42}
$$

Here, a_{if} represents the sum of the transition amplitudes a_{if}^n resulting from nth collision and with taking into account the phase shifts between amplitudes. Here N is the total number of nuclear collisions with the crystal atoms, $\gamma\varphi(\boldsymbol{r}(t))$ is the potential of the nth atom calculated in the nucleus rest frame, and $\mathcal{M}(\mathrm{E1}-\mu)$ is the standard defined [see, e.g. ref. [1]), p. 15] dipole matrix element and $\omega=(E_f-E_i)/\hbar$ is the transition frequency between nuclear levels.

If the nuclei in the initial beam are not polarized and no polarization measurements are made, the EE probability is to be averaged over the momentum projections in the initial states and to be summed over those in the final states. Using the Wigner-Eckart theorem for the tensor operator of the first rank and well-known orthogonality properties of the vector addition coefficients, the following expression for the E1 transition probability is obtained:

$$P_{if}(\mathrm{E1})=\frac{4\pi}{3\hbar^2}B(\mathrm{E1})\sum_{\mu=-1}^{1}\left|\sum_{n=1}^{N}\beta_\mu^n\right|^2=\frac{4\pi}{9\hbar^2}B(\mathrm{E1})\sum_{\alpha=1}^{3}\left|S_{\mathrm{E1}}^\alpha\right|^2. \tag{43}$$

Here $B(\mathrm{E1})$ is the standard reduced probability of the electric dipole transition [2]), and S_{E1}^α are the three components of the orbital integral for the total collision in the crystal:

$$S_{\mathrm{E1}}^1=\sum_{n=1}^{N}\exp\left(\frac{i\omega z_n}{\gamma v}\right)x_n\int_{-a/2}^{a/2}\frac{\mathrm{d}z}{v}\exp\left(\frac{i\omega z}{\gamma v}\right)\frac{1}{r}\frac{\partial}{\partial r}\varphi(r=\sqrt{x_n^2+y_n^2+z^2}),$$

$$S_{\mathrm{E1}}^2=\sum_{n=1}^{N}\exp\left(\frac{i\omega z_n}{\gamma v}\right)y_n\int_{-a/2}^{a/2}\frac{\mathrm{d}z}{v}\exp\left(\frac{i\omega z}{\gamma v}\right)\frac{1}{r}\frac{\partial}{\partial r}\varphi(r=\sqrt{x_n^2+y_n^2+z^2}), \tag{44}$$

$$S_{\mathrm{E1}}^3=\sum_{n=1}^{N}\exp\left(\frac{i\omega z_n}{\gamma v}\right)\frac{1}{\gamma}\int_{-a/2}^{a/2}\frac{\mathrm{d}z}{v}z\exp\left(\frac{i\omega z}{\gamma v}\right)\frac{1}{r}\frac{\partial}{\partial r}\varphi(r=\sqrt{x_n^2+y_n^2+z^2}). \tag{45}$$

The partial integration involved in going from (42) to (45) requires the fact that $\varphi(a/2)$ is small. The orbital integrals (44), (45) depend on x_n, y_n, z_n which are the coordinates of the point of the minimum distance between the nucleus and nth atom of the crystal. The OZ axis coincides here with the nearest crystallographic axis. The integration is performed in the laboratory frame along the trajectory defined by computer simulation, which leads to the knowledge of all values x_n, y_n, z_n.

The obtained expression (43) is to be averaged over all possible trajectories according to the initial conditions:

$$\langle P_{if}(\mathrm{E1})\rangle=\frac{1}{M}\sum_{m=1}^{M}P_{if}^m(\mathrm{E1})\Phi(\boldsymbol{r}_m(0),\boldsymbol{v}_m(0)), \tag{46}$$

where $P_{if}^m(\mathrm{E1})$ is the EE probability for the nucleus passing through the crystal along the mth trajectory defined by the point of incidence $\boldsymbol{r}_m(0)$ and the initial velocity $\boldsymbol{v}_m(0)$, and $\Phi(\boldsymbol{r}_m(0),\boldsymbol{v}_m(0))$ is the number of nuclei with those initial conditions.

The results of computer simulation are presented below for the concrete case of EE of the 110 keV level in the fluorine nucleus passing through a gold crystal. As

is shown in sect. 3, the straight-line approximation leads to sharp resonances in the EE probability for definite γ-values, namely when $\xi = \omega/\gamma v = 2\pi n/a$. This is a consequence of the fact, that the amplitudes are adding in phase in (42) and (43) and the EE probability is then proportional to the square of the number of collisions N^2.

The computer simulation allows one to understand how the shape and the magnitude of the resonance change when one deals with real trajectories instead of the straight-line ones. Fig. 8 represents the results of a computer simulation of the EE probability in the crystal for the same incident conditions, as in fig. 3b. Fig. 8a shows the results of a computer simulation with $M = 400$ nuclei and fig. 8b - the same with $M = 900$ nuclei. The crystal thickness was $L = 0.3$ μm which corresponds to $N = 10^3$ collisions. The EE probability for every trajectory was calculated using the formulae (43)-(45) and averaging (46) with the uniform distribution over points of incidence was done. From the comparison of fig. 3b and fig. 8a, b it follows that the bending of trajectories leads to dramatic broadening of the resonance and the maximum value of the EE probability is approximately less by an order of magnitude than in fig. 3b, calculated with the straight-line trajectories.

In comparing figs. 3b and 8b, the observed reduction is completely due to curvature of trajectories, because we consider here a rather thin crystal, where the nuclei collide only with separate (or several) atomic strings, and therefore the reduction is not caused by a non-uniform ion-flux, typical for various channeling problems [8]).

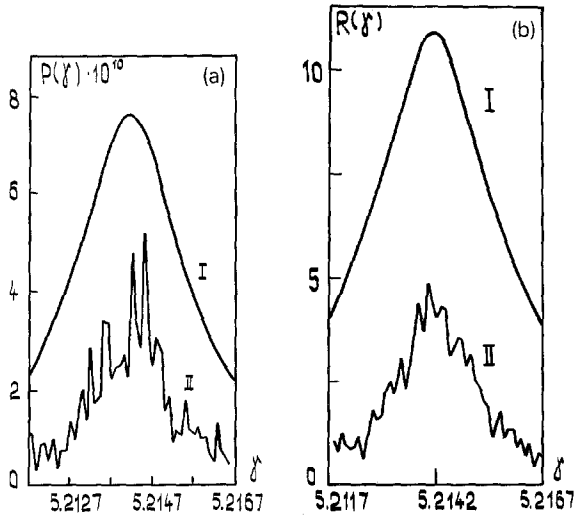

Fig. 8. Computer simulation results for the dependence of the EE probability $P(\gamma)$ of ^{19}F nuclei upon the Lorentz-factor γ near the resonance with $n = 5$ (as in fig. 3b) under (110) axial motion in Au with the statistics 400 (a) and 900 (b) nuclei. The upper curves in parts (a) and (b) are obtained for $T \approx 0$ and the lower ones for $T = 293$ K. In part (a) are given the absolute values of $P(\gamma)$ and in fig. (b) - the ratio $R(\gamma)$, the same as in fig. 3b.

The results given in fig. 8a, b are obtained for the case when the nuclei are passing near the separate atomic string in the crystal, i.e. $L \approx L_1$. The computer simulation shows that at $L > L_1$ the nuclei are interacting with several atomic strings during the penetration through the crystal. As a result, the nuclear trajectories turn out to be more complicated and various interference effects between the amplitudes corresponding to different strings are possible. This leads to oscillations in the thickness dependence of the EE probability $P_{if}(E1)$ and as a consequence, resonant behaviour like $P_{if} \sim N^2$ at $\xi = 2\pi n/a$ is not observed for $Na = L > L_1$ (the incidence velocity $v(0)$ was parallel to the atomic strings). On the contrary, when the incident angle between the velocity of the incident nucleus $v(0)$ and the atomic strings is not zero, but the velocity is parallel to the crystallographic planes (as in fig. 1b), the nuclear trajectories are quasiperiodic and are relatively stable in comparison with the axial channeling case. This kind of motion of nuclei between crystallographic planes is called planar channeling. The trajectories of this type lead to more ordered addition of the amplitudes from the different atomic strings. The resonant condition for this case depends on the crystal structure factor and for the case considered below, the (100) planar channeling in a gold crystal, is $\xi = 2\pi n \cos\theta/a$ with $n = 1, 3, 5, \ldots$ and θ being the angle between the initial velocity and the ⟨110⟩ axis. The $n = 1, 3, 5, \ldots$ values are characteristic for the face-centered lattice and (110) and (100) planar channeling.

Indeed, the computer simulation results confirm the suggestion about the advantages of the planar channeling. Fig. 9a shows a typical trajectory of a nucleus under (100) planar channeling and fig. 9b represents the EE probability of the nucleus ^{19}F

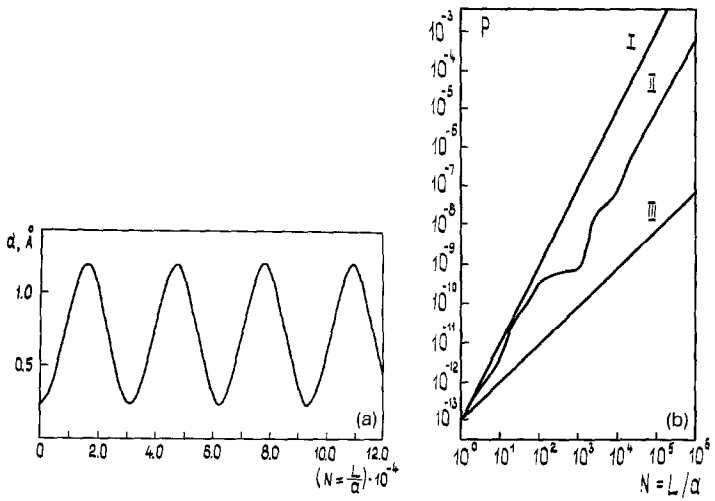

Fig. 9. (a) Projection of the typical planar channeled trajectory of nucleus in the (100) Au planar channel (the angle between $v(0)$ and ⟨110⟩ axis is $\theta = 10^{-3}$). The value $\gamma = 25.6$ is chosen and that is the condition for resonance with $n = 1$. (b) Dependence of the EE probability upon the crystal thickness for the simulated trajectory in part (a), curve II (see the details in text).

passing along this trajectory in terms of dependence on the collision number in the crystal (curve II). For comparison, two characteristic dependences, $P_{if}(N) \sim N^2 P_{if}(1)$ (curve I) and $P_{if}(N) \sim N P_{if}(1)$ (curve III) are given. Curve I corresponds to the case of "pure" resonance with the N^2 dependence, typical for the straight-line trajectories, and curve III corresponds (qualitatively) to the case of an amorphous target, with characteristic linear dependence on N. The behaviour of curve II leads to the conclusion about the constructive interference of the EE amplitudes corresponding to the different atomic strings, i.e. about the resonant EE under planar channeling of nuclei in the crystal. As follows from fig. 9b, at $N = 10^6$ (the corresponding crystal thickness is $L \approx 300$ μm) the EE probability of the projectile nucleus in the crystal reached a rather high value $P \approx 10^{-4}$ and that is the favourable case for the experimental investigation of this phenomenon.

Thus, the developed method of the computer simulation leads to the conclusion that the effect of the coherent resonant EE of relativistic nuclei in crystals occurs even if we take into account the difference between the straight-line trajectories and the real ones. The computer simulation results show that the more favourable case, from the point of view of possible experiment, is probably the planar channeling case. We suppose to provide the complete analysis of the EE under planar channeling in a separate paper, after obtaining the necessary statistics. In any way, our preliminary computer simulation results lead to the greater value of coherent EE probability in comparison with those obtained without taking into account the constructive interference between the separate-string amplitudes [23]).

Finally, we considered here a gold crystal in comparison with a thick diamond one in ref. [23]), because our purpose was to estimate the effect of coherent EE in a thin crystal and to obtain a greater value of the EE probability, which is proportional to Z^2 of a target. On the other hand, a thin gold crystal was used in successful experiments on coherent excitation of electronic levels of channeling ions [20]), therefore one can compare the atomic and nuclear effects of coherent excitation in the same crystal. If would be very interesting to provide computer simulation of this effect in thick silicon and germanium, which have Z greater then diamond and which are often used in channeling studies due to high quality of samples.

6. Conclusion

A theoretical analysis of the energy dependence of coherent EE and ED in the crystal is provided. The main results are as follows. There exist at $L > L_{ex}$ sharp resonances in the EE probability of the projectile relativistic nuclei passing through the crystals, at the definite γ-values, and only the broad maximum in the ED probability calculated as a function of γ. At $L < L_{ex}$ the characteristic increase of the EE and ED cross sections in the crystal is observed, which is connected with the coherent addition of the amplitudes at very high energies. The width and the magnitude of the resonances in EE change sufficiently when taking into account

the bending of the nuclear trajectories by means of computer simulation. These results lead to the conclusion about the possibility of the experimental investigation of resonant EE of relativistic nuclei in crystals.

It is necessary to note that the possible applications of the processes considered here are relativistic neutron (antineutron) generation via deuteron (antideuteron) coherent ED, or monochromatic photon generation via coherent EE. The shape of the VP spectrum (fig. 2) with the position of maxima determined by the γ-value is probably of interest for the nuclei spectroscopy or for the spectroscopy of compound elementary particles.

We are grateful to A. Winther for comments about the validity of the virtual photon method for EE problems. We are grateful to V.V. Okorokov and M.I. Podgoretsky for the helpful discussions and to R. Fusina and J.C. Kimball for the presentation of the paper [23]) before its publication. One of the authors (Y.L.P) wishes to thank J.U. Lindhard for useful discussion, and to thank the Niels Bohr Institute, where this work was completed, for the warm hospitality extended to him.

Note added in proof: Various reasons (bending of the trajectories, damping processes, energy loss processes, the calculation without using the perturbation theory, etc.) can lead to the break of the effect of the full coherence which appeared in sect. 3 as a consequence of the straight-line trajectories approximation and perturbation theory. Therefore, the N^2-dependence (see fig. 3a and sect. 3) is a very idealized case which appears only in the frame of this simplified model.

References

1) K. Alder and A. Winther, Electromagnetic excitation (North-Holland, Amsterdam, 1975)
2) A. Winther and K. Alder, Nucl. Phys. **A319** (1979)518
3. D.L. Olson, B.L. Berman, D.E. Greiner *et al.*, Phys. Rev. **C24** (1981) 1529
4. M.T. Mercier, J.C. Hill, F.K. Wohn *et al.*, Phys. Rev. **C33** (1986) 1655
4. C. Cohen, J. Dural, M.J. Gaillard *et al.*, J. Phys. **46** (1985) 1565
6. V.V. Beloshitsky and F.F. Komarov, Phys. Reports **93** (1982) 119
7) N. Cue and J.C. Kimball, Phys. Reports **125** (1985) 69
8) D.S. Gemmel, Rev. Mod. Phys. **46** (1974) 129
9) Yu.L. Pivovarov, V.G. Khlabutin and S.A. Vorobiev, Phys. Lett. **A76** (1980) 339; JETP Lett. **31** (1980) 199
10) M.L. Ter-Mikaelian, High energy electromagnetic processes in condensed media (Wiley, New York, 1972)
11) V.V. Okorokov, JETP Lett. **2** (1965) 111
12) V.V. Okorokov, Sov. J. Nucl. Phys. **2** (1965) 719
13) S. Shindo and Y.H. Ohtsuki, Phys. Rev. **B14** (1976) 3925
14) H. Crawford and R.H. Ritchie, Phys. Rev. **A20** (1979) 1848
15) V.A. Bazylev and N.K. Zhevago, Zh. Exp. Teor. Fiz. **77** (1979) 312
16) Yu.L. Pivovarov and S.A. Vorobiev, Dokl. Akad. Nauk SSSR **25** (1981) 837
17) Yu.L. Pivovarov and A.A. Shirokov, Yad. Fiz. **37** (1983) 1101 (Sov. J. Nucl. Phys. **37** (1983) 653)

18) Yu.L. Pivovarov, A.A. Shirokov, S.A. Vorobiev, Dokl. Akad. Nauk SSSR **272** (1983) 86 (Sov. Phys. Dokl. **28** (1983) 753)
19) Yu.L. Pivovarov and A.A. Shirokov, Yad. Fiz. **44** (1986) 882 (Sov. J. Nucl. Phys. **44** (1986) 569)
20) D.D. Miller *et al.*, Nucl. Instr. Meth. **B13** (1986) 56
21) B. Hoffmann and G. Baur, Phys. Rev. **C30** (1984) 274
22) J.D. Jackson, Classical electrodynamics (Wiley, New York, 1975)
23) R. Fusina and J.C. Kimball, Nucl. Instr. Meth. **B27** (1987) 368 and erratum to be published
24) P.A. Doyle and P.S. Turner, Acta Cryst. **A24** (1968) 390
25) G.E. Brown and A.D. Jackson, The nucleon-nucleon interactions (North-Holland, Amsterdam, 1976)
26) J.H. Barrett, Phys. Rev. **B3** (1971) 1527
27) E.G. Vyatkin, Yu.L. Pivovarov and S.A. Vorobiev, Nucl. Phys. **B284** (1987) 509